Fighting Malaria

Huizing, Anja P; Mondal, Milon; Hirsch, Anna K H

Published in:
Journal of Medicinal Chemistry

DOI:
10.1021/jm5014133

Journal of Medicinal Chemistry

Perspective

pubs.acs.org/jmc

Fighting Malaria: Structure-Guided Discovery of Nonpeptidomimetic Plasmepsin Inhibitors

Miniperspective

Anja P. Huizing, Milon Mondal, and Anna K. H. Hirsch*

Stratingh Institute for Chemistry, University of Groningen, Nijenborgh 7, NL-9747 AG Groningen, The Netherlands

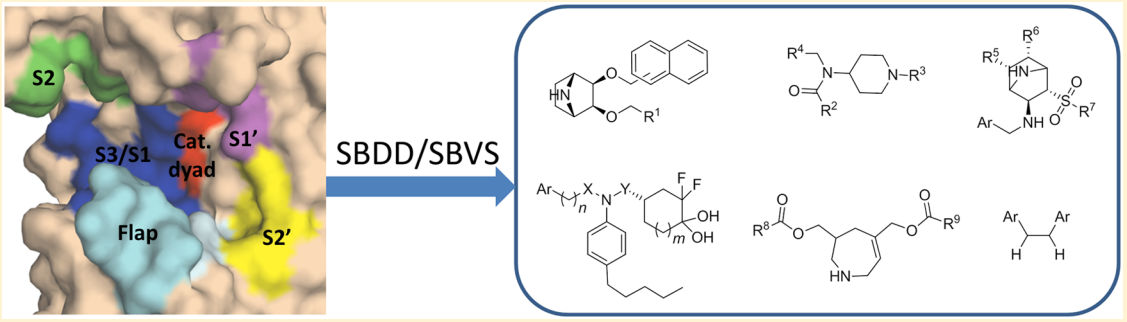

ABSTRACT: Plasmepsins (Plms) are aspartic proteases involved in the degradation of human hemoglobin by *Plasmodium falciparum*. Given that the parasite needs the resulting amino acid building blocks for its growth and development, plasmepsins are an important antimalarial drug target. Over the past decade, tremendous progress has been achieved in the development of inhibitors of plasmepsin using two strategies: structure-based drug design (SBDD) and structure-based virtual screening (SBVS). Herein, we review the inhibitors of Plms I–IV developed by SBDD or SBVS with a particular focus on obtaining selectivity versus the human Asp proteases cathepsins and renin and activity in cell-based assays. By use of SBDD, the flap pocket of Plm II has been discovered and constitutes a convenient handle to obtain selectivity. In SBVS, activity against Plms I–IV and selectivity versus cathepsins are not always taken into account. A combination of SBVS, SBDD, and molecular dynamics simulations opens up opportunities for future design cycles.

1. INTRODUCTION

Malaria is caused by parasites of the genus *Plasmodium* and constitutes a large threat to human health.[1] Of the four species of *Plasmodium* parasites, *P. vivax*, *P. ovale*, *P. malariae*, and *P. falciparum*, the last is the most lethal human pathogen. Several drugs and insecticides have been developed to prevent or treat malaria caused by *P. falciparum*, but increasing resistance against these treatments has stimulated the search and development of drugs with a novel mode of action.[2−6] The life cycle of *P. falciparum* involves three stages: the mosquito, liver (pre-erythrocytic), and blood (erythrocytic) stages of which the blood and liver stages take place in the human body. Most symptoms of malaria manifest themselves when the developing parasites (merozoites) are released from the liver into the bloodstream and invade red blood cells. Inside the red blood cells, the parasite degrades human hemoglobin in the food vacuole to produce amino acids for development and reproduction. These amino acids are essential for the growth and development of *P. falciparum*.[7−12] A class of eukaryotic Asp proteases of *P. falciparum*, plasmepsins (Plms) are involved in this process and are currently under investigation as drug targets.[13−16]

1.1. Plasmepsins. Ten types of Plms have been identified (I, II, III (HAP), IV, V, VI, VII, VIII, IX, and X),[13] fulfilling various functions in the development of *P. falciparum*. Plms I–IV are the most studied isoforms owing to their expression and important role during the blood stage. The vacuolar Plms I–IV are present in the food vacuole, are responsible for the proteolysis of hemoglobin, and display high sequence similarity (50–79%).[16−19] Inhibition and knockout studies have shown that inhibition of Plms I–IV kills the *P. falciparum* parasite and inhibition of any one of them is not sufficient.[20−23] As a result, these Plms have attracted much attention as potential drug targets, with Plm II being the best studied isoform. Structure-based drug design (SBDD) of inhibitors for Plm generally focuses on Plm II given that it was the first Plm for which a crystal structure became available.[17] Whereas Plm II still remains the best studied isozyme, Plms V–X remain considerably less understood; recent studies show that Plm V functions as *Plasmodium* export element (PEXEL) cleaving protease for protein export from the food vacuole to the erythrocyte to enable the development of *P. falciparum* parasites.[24,25] First inhibition studies indicate that Plm V could also serve as a drug target;[25] however, we will not cover these preliminary data in this review.

1.2. Structure of Plm II. Plms are similar in topology and shape to other Asp proteases (crystal structure and residues of

Received: September 15, 2014
Published: February 26, 2015

DOI: 10.1021/jm5014133
J. Med. Chem. 2015, 58, 5151−5163

a)

Asp dyad	Flap pocket	S1/S3	S2	S1′	S2′
Asp214, Asp34.	Pro43, Trp41, Met75, Val82, Val105, Thr108, Phe111, Ile123.	Ile14, Met15, Phe16, Tyr17, Ile32, Phe111, Thr114, Phe120, Ile123, Ser215, Gly216, Thr217, Ser218.	Ala219, Pro243, Phe244, Leu271, Tyr273, Met286, Asn288, Ile289, Ile290.	Tyr192, Trp193, Ile212, Phe294, Ile300.	Ala38, Asn39, Leu131, Ser132, Ile133.

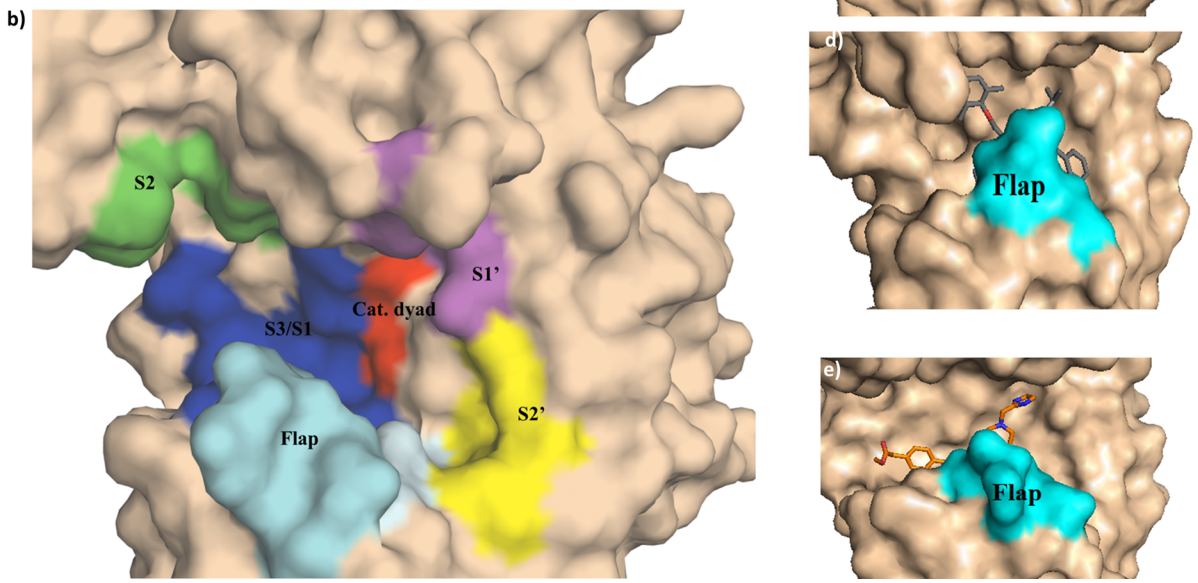

Figure 1. Plm II crystal structures. (a) List of important amino acid residues lining the respective pockets.[32] (b) Representation of the pockets (PDB code 2BJU),[37] named according to Schechter.[30] (c–e) Representations of three conformations of the flap, from top to bottom: closed (PDB code 1SME), slightly open (PDB code 1LEE), and open (PDB code 2BJU).

Plm II are displayed in Figure 1a,b), including human Asp proteases and HIV-1 protease. Asp proteases contain a single peptide chain that is folded into two domains (C- and N-terminal), which in turn are connected along the bottom of the binding cleft via the catalytic dyad.[26] Features of Plms I–IV include the acidic catalytic dyad (Asp34 and Asp214; pH ≈ 5),[27] which contains one deprotonated Asp residue for proton transfer during the hydrolysis of hemoglobin[28] and a β-hairpin turn, the flap (residues 76–84), which covers the catalytic dyad and interacts with the substrate.[26,29] Structural analysis of Plm II in complex with various classes of inhibitors revealed this flap to be highly flexible, adopting three different conformations (Figure 1c–e). Even though less information is available for Plms I, III, and IV, it is assumed that their flaps display similar flexibility. As will be shown in this review, structure–activity relationships (SARs) do not always support this. Detailed analysis of Plm II enabled the identification of several lipophilic pockets (S3–S2′ and a flap pocket)[30−32] surrounding the active site, which can host the inhibitors.

The RCSB Protein Data Bank (PDB) currently contains 15 X-ray cocrystal structures of Plm II in three distinct flap conformations.[33] Nine crystal structures of Plm II are in complex with pepstatin-derived inhibitors in a closed flap conformation (PDB codes 1SME, 1M43, 1ME6, 1XDH, 1XE5, 1XE6, 1W6H, 1W6I, and 2R9B),[17,34] three with peptidomimetic inhibitors in a more open flap conformation (PDB codes 1LEE,[35] 1LF2,[35] and 1LF3[36]), and three with achiral piperidine inhibitors in an open flap conformation (PDB codes 2BJU,[37] 2IGX,[38] and 2IGY[38]). The final group is available since 2005 and are the only structures where the flap pocket can be used for modeling studies, important for SBDD.

Reviews have been published where expression and crystallization methods,[39] development of Plm II antimalarial agents,[5,6,20,40−42] and computational methods[43] for Plm-inhibitor design have been discussed. This review covers SBDD and virtual screening (VS) approaches using crystal structures of Plm II for the development of nonpeptidomimetic Plm inhibitors. Important progress regarding the activity and selectivity of Plm II inhibitors will be invaluable for future development of Plm inhibitors.

Criteria for promising candidates are inhibition of Plm II, preferably also Plms I–IV and activity against *P. falciparum* (IC_{50} < 1 μM). Owing to the similarity of Plm II with the human Asp proteases cathepsin (Cat) D/E and renin, a Plm II inhibitor should show selective inhibition over these human Asp proteases (30–35% similarity to Plm II).[17,19]

2. STRUCTURE-BASED DRUG DESIGN

In 1996, the first X-ray crystal structure of Plm II in complex with pepstatin A was published (PDB code 1SME).[17] It was used for SBDD by the F. Diederich group in 2002,[44] taking inspiration from a 3,4-disubstituted piperidine, reported as an inhibitor of human renin.[45]

2.1. Azacyclic Scaffold. F. Diederich and co-workers identified the pockets of Plm II to be used for SBDD using both a closed conformation of Plm II (PDB code 1SME) and an open flap conformation of human renin (EC 3.4.23.15).[44,46] Given that Plm II is highly flexible, it was assumed that similar conformations could be adopted by Plm II. Consequently, the renin structure in the open-flap conformation was used to

DOI: 10.1021/jm5014133
J. Med. Chem. 2015, 58, 5151−5163

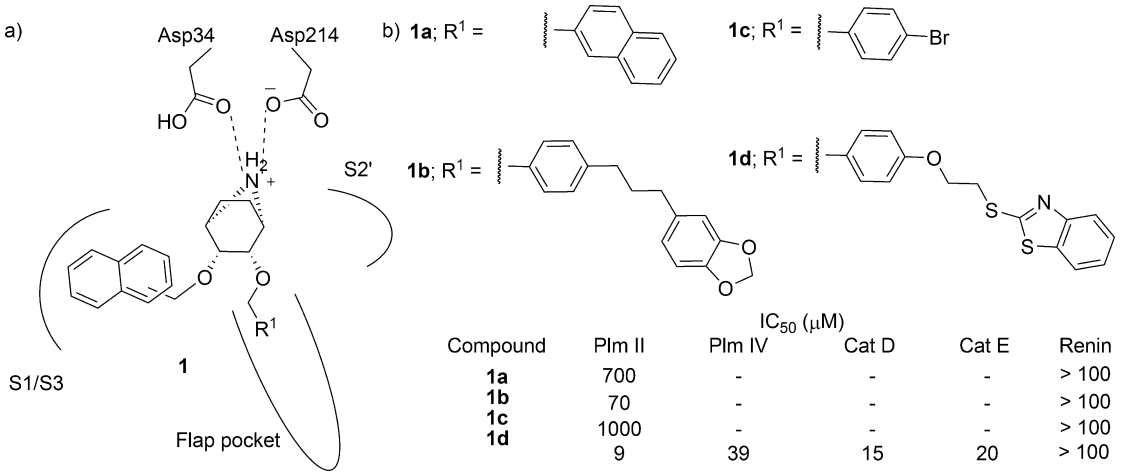

Compound	IC_{50} (μM) Plm II	Plm IV	Cat D	Cat E	Renin
1a	700	-	-	-	> 100
1b	70	-	-	-	> 100
1c	1000	-	-	-	> 100
1d	9	39	15	20	> 100

Figure 2. First generation of azacyclic inhibitors reported by F. Diederich and co-workers: (a) schematic representation of the binding mode of inhibitor **1**; (b) structures and biochemical activity of first-generation inhibitors investigated.[46]

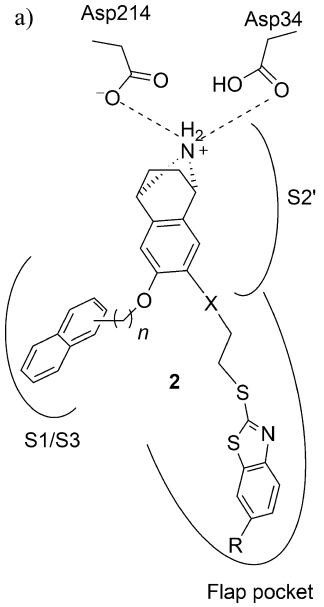

Compound	X	R	*n*	naphthyl	IC_{50} values (μM) Plm II	Plm IV	Cat D	Cat E	Renin
2a	O	H	2	1-	13	60	18	34	83
2b	O	H	1	2-	10	85	23	42	81
2c	O	H	1	1-	14	70	25	46	> 100
2d	O	Cl	2	1-	3	15	12	6	> 100
2e	O	Cl	1	2-	4	50	11	14	> 100
2f	O	Cl	1	1-	5	17	12	7	> 100
2g	CH_2	H	1	1-	4	33	12	9	93
2h	CH_2	Cl	1	1-	2	10	7	4	> 100

Figure 3. Second generation azacyclic inhibitors reported by F. Diederich and co-workers: (a) schematic representation of the binding mode of the second-generation inhibitor **2**; (b) structures and biochemical activity of second-generation inhibitors investigated.[44,47]

explore the additional space for modeling. A S1/S3, a S2′, and a flap pocket were identified based on the structure of renin and were used for modeling studies, even though no evidence existed yet for the presence of a flap pocket in Plm II.

A first generation of inhibitors consisted of an azanorbornene in which the protonated azacyclic group (pK_a = 10.8) was proposed to interact with the catalytic dyad at pH = 5 (**1**, Figure 2a).[46] The scaffold contains two substituents: a naphthyl group, which according to modeling, was suggested to establish van der Waals contacts with Met15, Phe111, and Phe120 of the S1/S3 pocket or Leu131 and Tyr192 of the S2′ pocket depending on the enantiomer, and a heteroaromatic group, which was suggested to interact with Val105 and Tyr115 of the flap pocket (Figure 2a). Inhibitor **1** featuring various R^1-substituents (**1a**–**d**) showed micromolar Plm II activity, high selectivity versus human renin, and no selectivity versus Cat D/E (**1d**, Figure 2b). Changing the connectivity of the naphthyl substituent did not affect activity, suggesting that the S1/S3 pocket is sufficiently large to host to these substituents.

The high flexibility of this first generation of inhibitors was thought to cause the low Plm II activity, which is why a more rigid azatricyclic scaffold **2** (Figure 3a), accessible via a shorter and more efficient synthetic route, was designed to shorten the linker to the substituent.[44,47] Initial inhibitor designs (**2a**–**c**, Figure 3b) neither showed improved activity nor higher selectivity versus Cat D/E compared to the first generation of inhibitors. Modeling studies indicated that introduction of a chlorine substituent at the benzothiazolyl ring could lead to enhanced activity, which was the case (**2d**–**f**). Conformational analysis and computational studies suggested a more favorable conformation of the inhibitor with X = CH_2, but this still led to micromolar activity (**2g**–**h**). Focusing on better occupancy of the large flap pocket, a larger R^1 substituent was introduced (**2**, with a phenyloxadiazolyl instead of benzothiazolyl). The decreased Plm activity observed illustrates the size limits of this substituent. Despite all efforts, second-generation compounds **2** did not display enhanced activity or selectivity compared to first-generation compounds (**1**).

DOI: 10.1021/jm5014133
J. Med. Chem. 2015, 58, 5151−5163

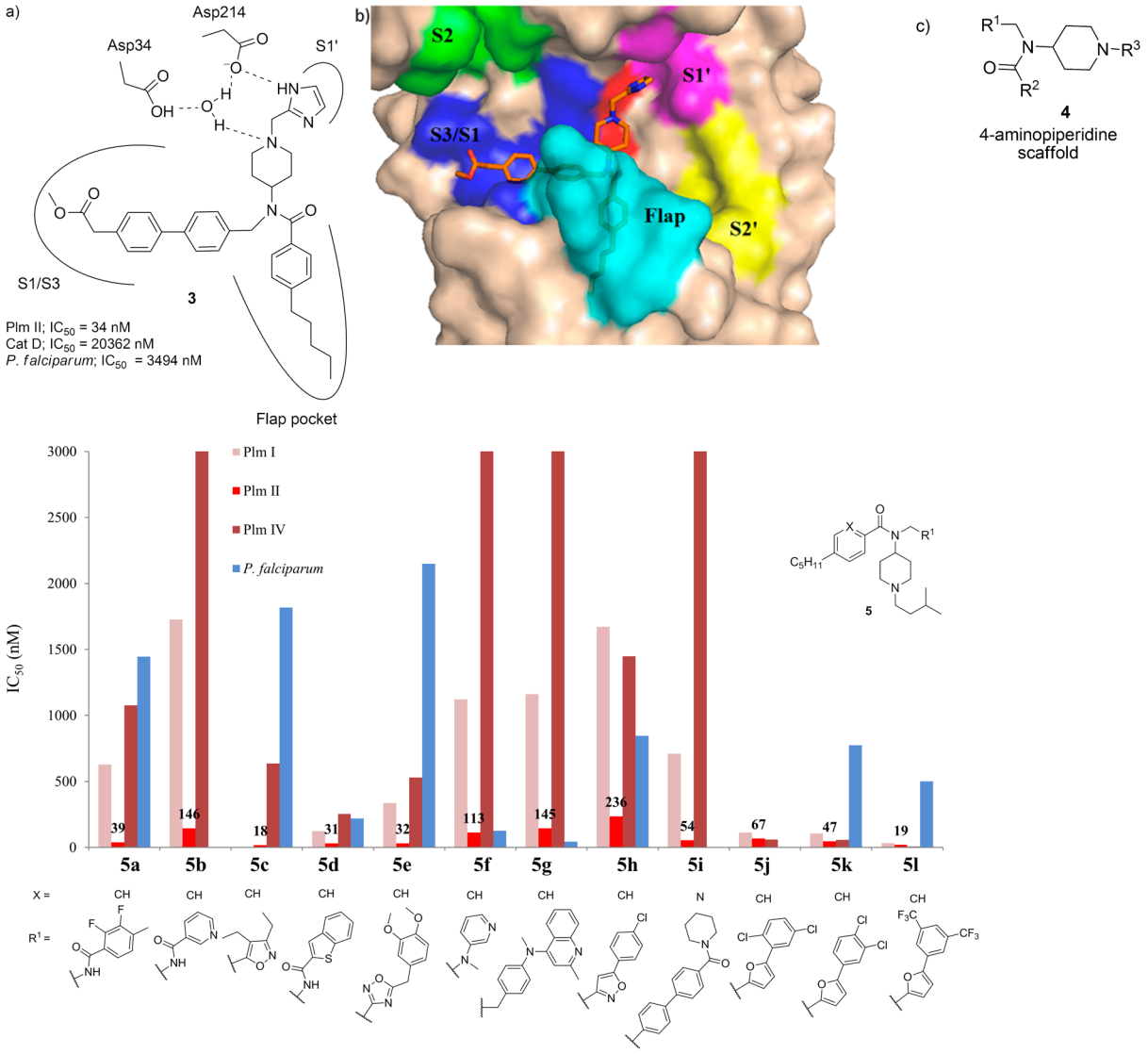

Figure 4. Achiral aminopiperidine inhibitors reported by Prade et al.:[27,34] (a) schematic representation of the binding mode of inhibitor **3**; (b) crystal structure of **3** in complex with Plm II; (c) representation of the basic scaffold **4**; (d) structures and biochemical activity ranges of inhibitor series **5** with IC_{50} values for Plm II displayed.[37,38]

2.2. Plm II Crystal Structure with Open Flap. In 2005, Prade et al. identified by high-throughput screening (HTS) an achiral 4-aminopiperidine, a known inhibitor of HIV-1 protease, with excellent Plm II activity (**3**, Figure 4a, Plm II IC_{50} = 34 nM) and high selectivity versus Cat D.[37] The crystal structure of Plm II in complex with compound **3** (PDB code 2BJU) revealed an open-flap conformation with access to a new flap pocket useful for inhibitor design (Figure 4b). Using this crystal structure, Prade et al. designed a series of easily synthesizable, achiral Plm II inhibitors featuring a 4-aminopiperidine scaffold (**4**, Figure 4c).[38] The aminopiperidine scaffold was designed to make a H-bonding interaction with the catalytic water molecule, and the three substituents (R^1, R^2, and R^3) are expected to interact with the S1/S3/S5, flap, and S1′ pockets, respectively, by analogy to compound **3** (Figure 4b). Modeling demonstrated the importance of the R^2 = 4-*n*-pentylphenyl substituent of which the *n*-pentyl chain fills the flap pocket, also visible in the crystal structure of **3** in complex with Plm II (Figure 4b).

Given that all compounds with the *n*-pentyl substituent occupying the flap pocket were found to be selective versus Cat D and E as well as human renin, this substituent was established to be essential for selectivity versus Cat D/E. Room for improvement was found for the other two substituents, with indications that the S1′ pocket would be better suited to host a more hydrophobic alkyl chain (R^3). Replacing the imidazolyl (R^3) by a more hydrophobic 4-pentyl group only led to enhanced Plm II activity. The scaffold with these R^2 and R^3 substituents was used for further exploration of variations in R^1 (scaffold **5**). This led to a series of inhibitors (**5a**–**i**) without clear SAR data (Figure 4d). Hence, models of Plms I and IV based on Plm II were used to enhance the activity against Plms I–IV. Given that efforts to optimize **5** were unsuccessful, a cocrystal structure of Plm II in complex with **5i** was solved in order to elucidate the binding mode. Conformational changes in the S1/S3 pocket affecting its size and shape were observed, suggesting the benzyl ring in **5i** can be optimized. Furanyl derivatives **5j**–**l** were found to display enhanced activity compared to the benzyl derivatives **5g** and **i**. Even though **5l** was the most active inhibitor of Plms I, II, and IV in vitro, it was much less active against *P. falciparum*. Surprisingly, the weaker inhibitor **5g** was found to be highly active against *P. falciparum* (Figure 4d).

DOI: 10.1021/jm5014133
J. Med. Chem. 2015, 58, 5151–5163

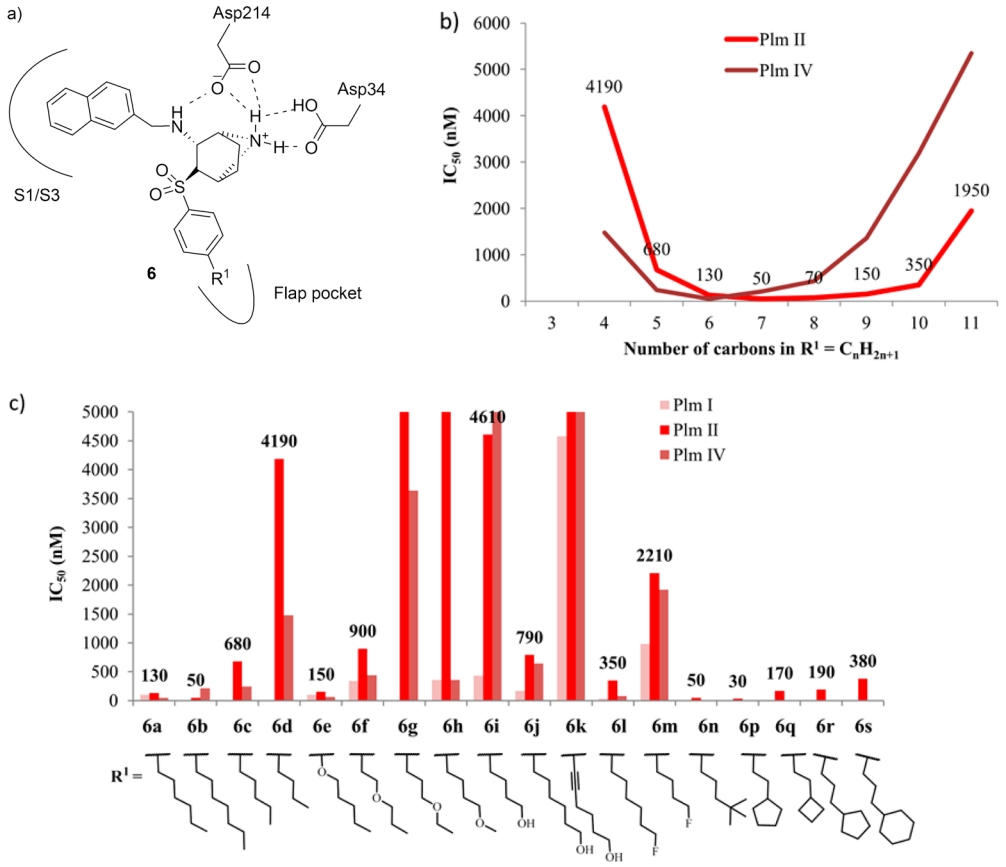

Figure 5. Azanorbornene arylsulfonyl inhibitors reported by F. Diederich and co-workers: (a) schematic representation of the binding mode of inhibitor **6**; (b) SAR of different alkyl-substituted derivatives of **6**; (c) structures and biochemical activity ranges of derivatives of **6**.[47−50]

2.3. Azanorbornene Diamine Clamp. In a follow-up of previous work, F. Diederich and co-workers designed an azanorbornene scaffold featuring an arylsulfonyl moiety and a basic "diamine clamp", enabling stronger interactions with the catalytic dyad (**6**, Figure 5a).[48−50] On the basis of the work of Prade et al., an R^1 = *n*-pentyl (Figure 5c) substituent was introduced to occupy the flap pocket, resulting in the expected selectivity versus Cat D/E and nanomolar activity against Plms I, II, and IV. This modification led to a significant improvement over previous inhibitors.[44−46] Optimization of R^1 by varying the alkyl lengths and/or substitution patterns (Figure 5b)[48] afforded SARs that reveal optimum activity for an *n*-heptyl substituent.[49] Subsequently, optimization of R^1 was performed by introduction of fluorine, ether, alkene, alkynol, or alcohol functionalities (Figure 5c).[50] Owing to the hydrophobicity of the flap pocket (Val105, Val82, Trp41, and Pro43), none of these derivatives displayed increased activity against Plms. Exploration of the aryl-favoring S1/S3 pocket showed the best results for naphthyl (**6**) and also for a *m*-bromophenyl-substituent, but in subsequent designs only the naphthyl substituent was used.

In 2013, F. Diederich and co-workers introduced a third substituent to their previous design (**6**) to improve Plm inhibition. A 5- or 6-substituted cycloalkyl group (**7**, Figure 6) was introduced and was suggested to interact with the Tyr192, Ile212, Phe294, and Ile300 residues of the S1′ pocket.[49]

Substitution at R^1 with cycloalkylamine groups mostly improved inhibition of Plm IV (**7a** and **7c**). This result cannot be explained by comparison of crystal structures of Plms I, II, and IV, which feature structurally conserved S1′ pockets. Substitution at R^2 showed lower, but still nanomolar, activity against the Plms, significantly increased selectivity versus Cat D and E (**7b** and **7c**) as well as an improved cell-based activity against *P. falciparum* (IC_{50} < 3 μM).

2.4. α,α-Difluoroketone Hydrate Scaffold. From a search for other scaffolds, α,α-difluoroketone hydrates emerged as a transition state isostere for aspartic proteases.[52] This scaffold was used for the design of new Plm inhibitors using a series of Plm structures in an open flap conformation (PDB codes 2IGX, 2IGY, and 2BJU).[53] Building on previous results, this inhibitor features naphthyl (S1/S3 pocket) and 4-pentylphenyl substituents (flap pocket) connected through an amide core (**8**, Figure 7a). A new alicyclic α,α-difluoroketone hydrate substituent was envisioned to function as a "clamp" involved in an H-bonding interaction with the catalytic dyad. The geminal fluorine atoms were suggested to be engaged in dipolar interactions with Gly36 and Gly216 (Figure 7a). All compounds with a cyclohexyl substituent (*m* = 1) (most active, **8a**,**b**) displayed micromolar IC_{50} values against Plm but low activity against Cat D/E (Figure 7b).

All compounds with cyclopentyl substituents (*m* = 0) showed decreased activity against Plms II and IV (IC_{50} > 100 μM), which could be ascribed to decreased hydrate formation. This hypothesis was confirmed by ^{19}F-NMR studies to determine the extent of hydrate formation for both cyclohexyl and cyclopentyl derivatives, showing almost full (>98%) and no conversion into the hydrate, respectively. To evaluate the importance of the α,α-difluoroketone hydrate, control experiments with monohydroxycyclopentyl, monohydroxycyclohexyl, and piperidinium analogues were performed, which resulted in inactive (IC_{50} > 100 μM), less active (IC_{50} = 20−24 μM), and

DOI: 10.1021/jm5014133
J. Med. Chem. 2015, 58, 5151−5163

a)

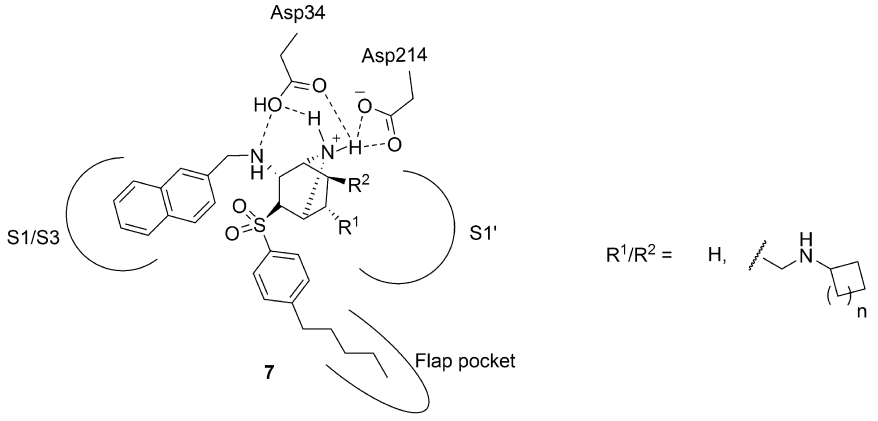

b)

IC_{50} values (nM)

	R^1	R^2	Plm I	Plm II	Plm IV	Cat D	Cat E	*P. falciparum* NF54
7			42–284	72–494	6–859	631–32100	811–> 100000	
7a	$n = 1$	H	89	72	18	3250	1940	2554
7b	H	$n = 1$	284	234	228	13700	> 100000	
7c	$n = 2$	H	100	107	11	1997	7547	829
7d	H	$n = 2$	289	198	139	6800	22300	

Figure 6. The 2,3,5- and 2,3,6-trisubstituted azanorbornene inhibitors reported by F. Diederich and co-workers: (a) schematic representation of the binding mode of inhibitor **7**; (b) structures and biochemical activity ranges of derivatives **7a–d**.[51]

a)

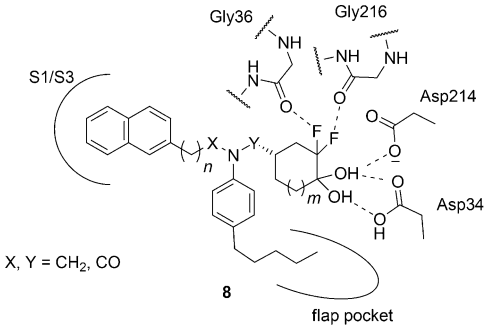

b)

IC_{50} values (μM)

	X	Y	*n*	*m*	Plm II	Plm IV	Cat D	Cat E
8					7–43	57–> 100	87–> 100	87–> 100
8a	CH_2	CO	0	1	10	73	> 100	> 100
8b	CO	CH_2	0	1	7	57	87	87

Figure 7. α,α-Difluoroketone hydrate inhibitors reported by F. Diederich and co-workers: (a) schematic representation of the binding mode of inhibitor **8**; (b) structures and biochemical activity ranges of derivatives **8**.[53]

similarly active inhibitors (IC_{50} = 13–19 μM), respectively. Taken together, it was shown that the cyclohexyl group is important for inhibition, but no significant improvement over an amine clamp has been achieved.

2.5. Azacycloheptene Scaffold. Inspired by the work of F. Diederich,[44,46–48] the group of W. E. Diederich reported in 2008 an azacycloheptene scaffold in a boat conformation with a protonated azepine functionality (**9**, Figure 8a) to address the catalytic dyad.[54] The approach of this group is different from previously described approaches, since the flap is used in modeling studies for possible interactions with the inhibitor. Modeling of the scaffold into three different flap conformations of Plm II (PDB codes 1SME (closed), 1LF2 (more open), and 2BJU (open flap)) suggested 3,5-substituents to interact with the S2′ and S1 pockets (Figure 8a). The ester functionalities were introduced primarily for synthetic feasibility and to be engaged in H-bonding interactions with flap residues Val78 and Ser79. To identify the most suitable substituent on the way to potent inhibitors, ligands for similar aspartic protease subsites were analyzed (Cavbase database).[54] This search suggested that similar S1 subsites prefer a phenyl moiety, but results for the S2′ pocket did not indicate preference for a specific class of substituents. To identify the best substituent for the S2′ pocket, a combinatorial VS approach of all commercially available carboxylic acids for both Plm II and IV was used. A fixed position of Asn39 in the crystal structure may have misguided the search by excluding H-bond acceptors, leading to compounds with low Plm affinity (best results for **9a** (IC_{50} = 6 μM)). Molecular dynamics (MD) simulations were used to introduce Plm II flexibility and showed Asn39 rotations allowing H-bond acceptors to form an H bond with the backbone N–H of Asn39. Remodeling suggested a *p*-bromophenyl S2′ substituent interacting with Asn39, Leu131, and Tyr192 and a *p*-phenylamine S1 substituent interacting with Met15, Tyr17, and Ser118 as featured by compound **9b**, which displays selectivity versus Cat D and improved Plm activity.[54] However, these compounds did not show significant improvement over the disubstituted azacyclic inhibitors reported previously (IC_{50} < 300 nM).[48–50]

2.6. Pyrrolidine Scaffold. Inspired by the design of pyrrolidine inhibitors for the related HIV-I protease,[55] a series of pyrrolidine-based Plm inhibitors was designed (**10** (symmetric), **11** (asymmetric), Figure 9a).[56] Interactions were expected to be similar to the azacycloheptene inhibitors:[54] a protonated pyrrolidine scaffold forms an H bond with the catalytic dyad, and ester or amide carbonyl oxygen atoms interact through H-bonding interactions with flap residues Ser79 and the backbone N–H of Val78 (Figure 9a), comparable to a closed flap conformation. Modeling of this scaffold into a closed flap conformation of Plm II (PDB code 1SME), however, was unsuccessful. Even modeling into a more spacious, opened

DOI: 10.1021/jm5014133
J. Med. Chem. 2015, 58, 5151–5163

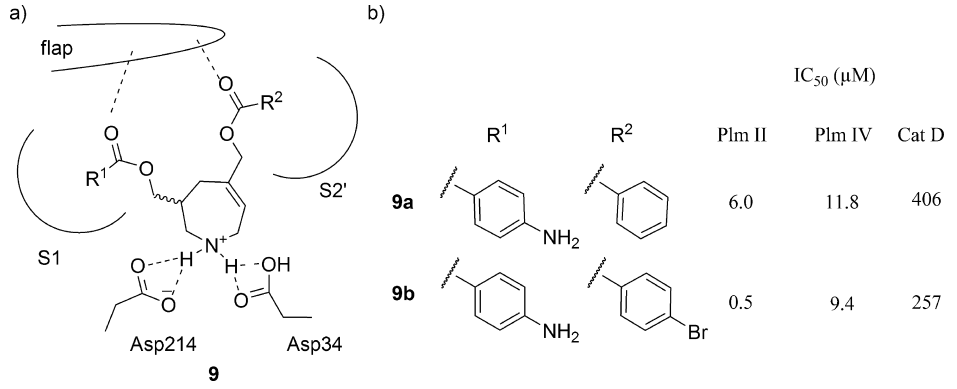

Figure 8. Azacycloheptene inhibitors reported by W. E. Diederich and co-workers: (a) schematic representation of the binding mode of inhibitor **9**; (b) structures and biochemical activity of derivatives **9a**,**b**.[54]

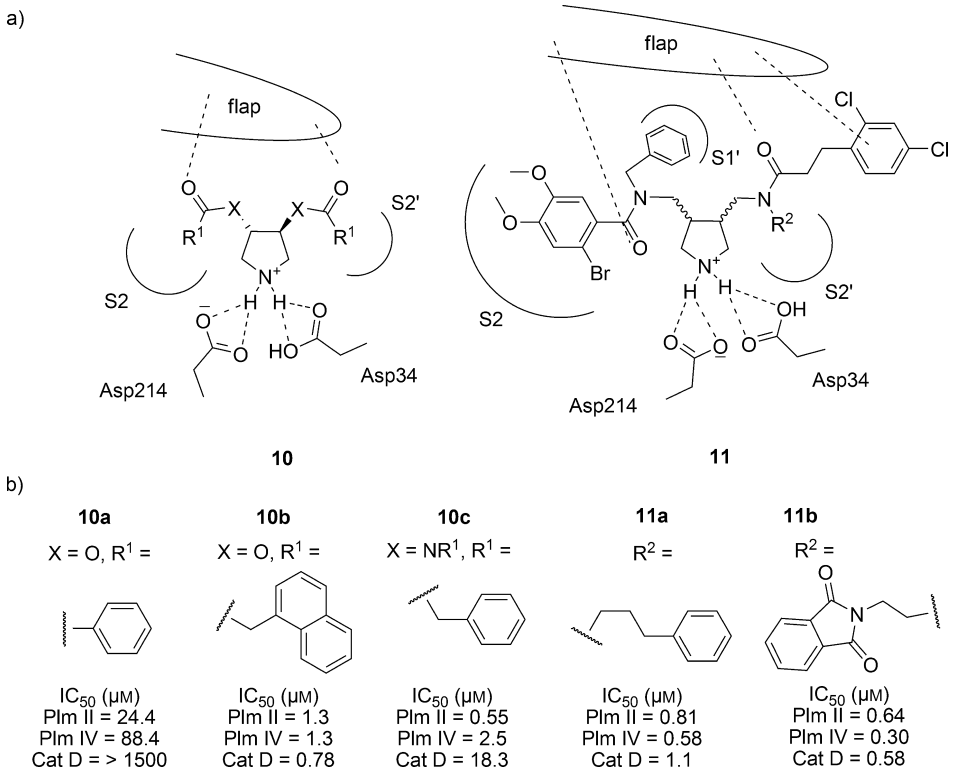

Figure 9. 3,4-Disubstituted pyrrolidine inhibitors reported by Klebe and co-workers: (a) schematic representation of the binding mode of inhibitors **10** and **11**; (b) structures and biochemical activity of **10** and **11**.[56]

conformation (PDB code 1LEE) was more difficult than expected. Again, introducing flexibility into Plm II with MD solved this problem and aromatic 3- and 4-substituents were found to interact with the S2 (Met15 and Ser218) and S2′ (Asn39 and Leu131) pockets (Figure 9a). Three classes of compounds were selected: symmetric esters (**10a**,**b**), amides (**10c**), and asymmetric amides (**11a**,**b**). With this design, however, the activity against Plms could not be optimized without a concomitant loss in selectivity versus Cat D.

3. STRUCTURE-BASED VIRTUAL SCREENING

3.1. WISDOM Project. A WISDOM (wide in silico docking on malaria) project was started in 2007 using a VS HTS approach.[57] The ZINC database of 3.3 million compounds was computationally screened with crystal structures of Plm II (PDB codes 1LEE and 1LF2) and Plm IV (PDB code 1LS5). Potential inhibitors were selected based on interactions with selected residues: Asp34 and Asp214 (catalytic dyad), Val78 and Ser79 (flap), and Ser218 and Gly36 (adjacent to catalytic dyad). A list of top-ranked compounds, featuring diverse scaffold structures such as thiourea, diphenylurea, and guanidino analogues, was obtained. Thiourea and diphenylurea analogues had been reported previously as potent micromolar inhibitors of Plms but lacking results from biochemical assays.[52] In 2009, a new publication of the WISDOM project appeared, with improved selection criteria for compounds and results from biochemical assays.[58] The binding modes of known inhibitors such as RS367, RS370 (Figure 10), and pepstatin A were analyzed to select the residues to be included for VS: Val78, Asp214, Asp34, Ser79, and Gly36. The top 200 compounds were selected and inspected visually and found to occupy the hydrophobic S1, S2, S1′, and S2′ pockets mainly with aromatic groups, stabilizing the protein−ligand complexes.

DOI: 10.1021/jm5014133
J. Med. Chem. 2015, 58, 5151−5163

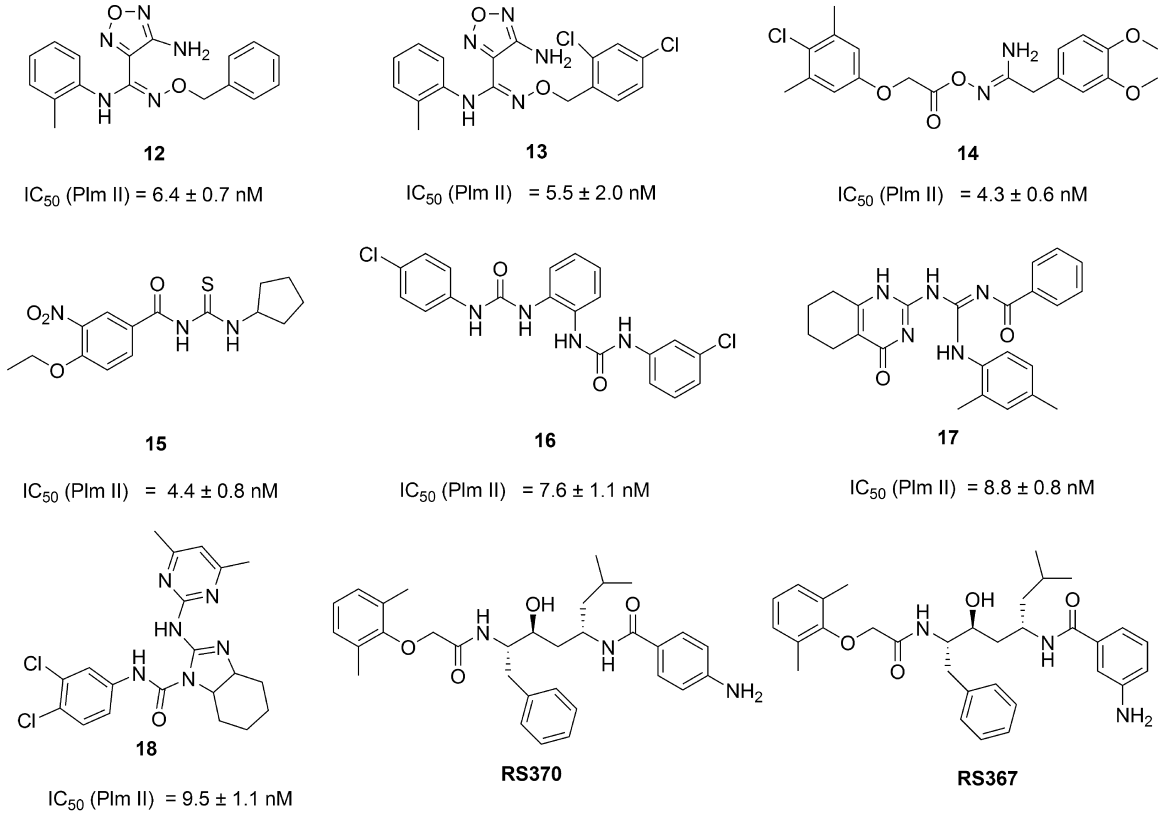

Figure 10. Seven Plm II inhibitors identified by VS.[58]

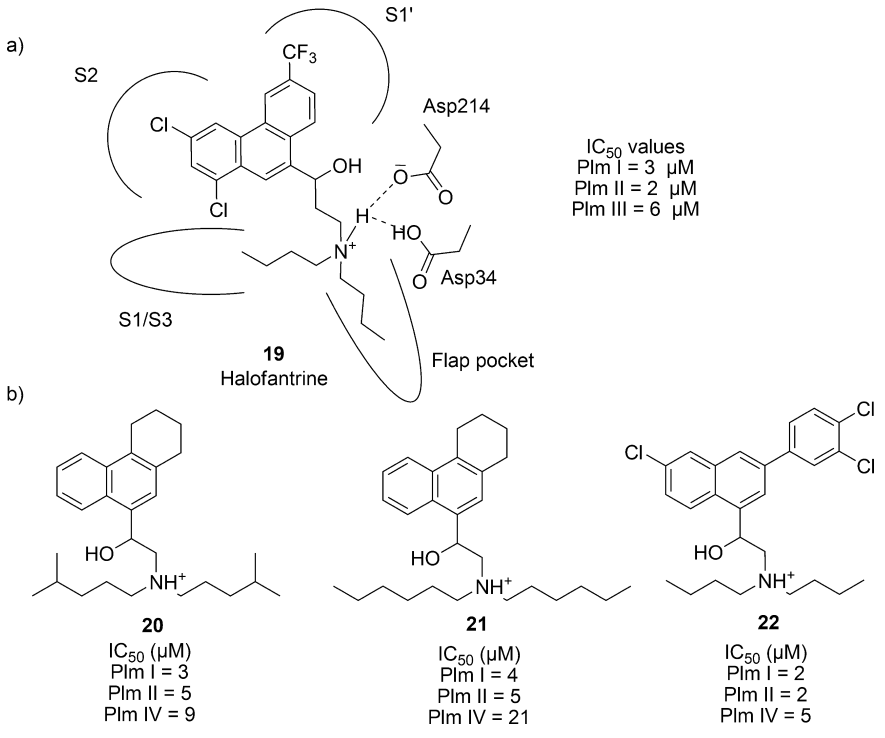

Figure 11. Amino alcohol inhibitors reported by Friedman and Caflisch:[59] (a) schematic representation of the binding mode of inhibitor **19**; (b) structures and biochemical activity of modified inhibitors **20**–**22**.[59]

The 200 compounds were divided into groups based on interactions with the catalytic dyad. Four types of cores were identified: *N*-alkoxyamidines, guanidines, amides, and ureas/thioureas. Thirty compounds were selected from these four classes, based on at least one additional interaction with Ala38 (S2′), Asn39 (S2′), Asn76 (flap), Tyr192 (S1′), and/or Thr217 (S1/S3). The compounds were tested against Plm II, which is not sufficient to claim activity against *P. falciparum* parasites; nevertheless,

DOI: 10.1021/jm5014133
J. Med. Chem. 2015, 58, 5151−5163

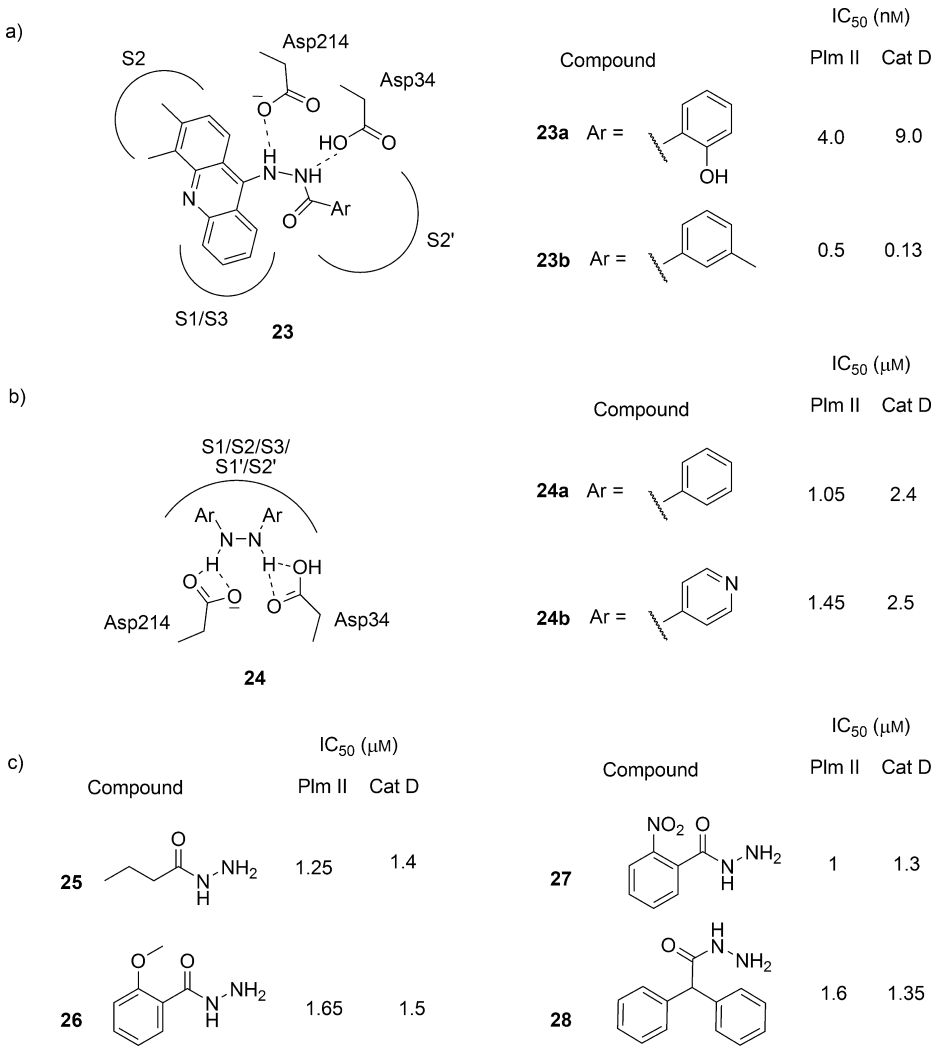

Figure 12. Hydrazide acridines[61] and hydrazides/hydrazines[63] inhibitors reported by Azim et al.: (a) schematic representation of the binding mode of inhibitor **23**, structures, and biochemical activities; (b) schematic representation of the binding mode of inhibitor **24**, structures, and biochemical activities; (c) structures and biochemical activities of derivatives **25**–**28**.

26 out of 30 compounds display nanomolar Plm II activity of which seven compounds display IC_{50} values of <10 nM (**12**–**18**; Figure 10). The binding mode of these compounds has not been reported.

3.2. Amino Alcohol Scaffold. In 2009, a Plm II LIECE (linear interaction energy with continuum electrostatics) model (PDB code 1LF3) was fitted from 20 known peptidic inhibitors.[59] Screening of the ZINC database resulted in 19 top-ranked compounds, which were tested against Plms I, II, and III (or IV). One of the three compounds featuring IC_{50} values of <5 μM against Plms I and II was halofantrine (**19**, Figure 11a),[60] a known antimalarial drug. Modeling studies of **19** were performed to derive a plausible binding mode, in which the isostere amino alcohol core interacts with the catalytic dyad and flap residue Ser79 through its protonated amine and its OH group, respectively.

Two long alkyl substituents are suggested to interact with the flap (Tyr77) and S1/S3 (Ile32, Thr114, Phe120, and Ile123) pockets. A partially aromatic cyclic substituent occupies the S2 (Thr217, Ser218, and Ile290) and S1′ pockets (Leu292 and Ile300) (Figure 11a). For the first time, an alkyl rather than an aromatic substituent was used to fill the S1/S3 pocket. A branched alkyl substituent does not influence the activity (**20** and **21**, Figure 10), but establishing whether the substituent accommodated in the S1/S3 pocket should be an alkyl or aromatic moiety could be useful for future design cycles. A substructure search based on the amino alcohol scaffold led to 40 new compounds of which only one (**22**) showed similar activity against Plms I, II, and III. In total, 13 compounds showed Plm inhibition (IC_{50} < 100 μM) of which nine are with an amino alcohol isostere scaffold.

3.3. Hydrazide and Hydrazine Scaffolds. Azim et al. performed VS of an in-house library using crystal structures of Plm II with pepstatin A (PDB code 1M43) and Cat D (PDB code 1LYB).[61] Two top-ranked acridine derivatives (**23a** and **23b**, Figure 12a) showed interactions of the hydrazine moiety (**23**, Figure 12a) with the catalytic dyad, of the acridinyl substituent with S1/S2/S3 (Ile32, Tyr77, Ile11, Ile123, Thr217, and Thr221) and of the phenyl substituent with flap (Met75, Asn76, and Tyr77) and S2′ (Leu131) residues. These compounds were tested against Plm II and Cat D, displaying single-digit nanomolar IC_{50} values in both cases. Because hydrazides/hydrazines had proven to inhibit Plms,[62] in 2010 Azim et al. repeated the VS of an in-house library of hydrazines/hydrazides, leading to two top-ranked low-molecular-weight hydrazine inhibitors (**24a**,**b**, Figure 12b), which showed interactions of the hydrazine moiety (**24**, Figure 12b) with the catalytic dyad,

DOI: 10.1021/jm5014133
J. Med. Chem. 2015, 58, 5151−5163

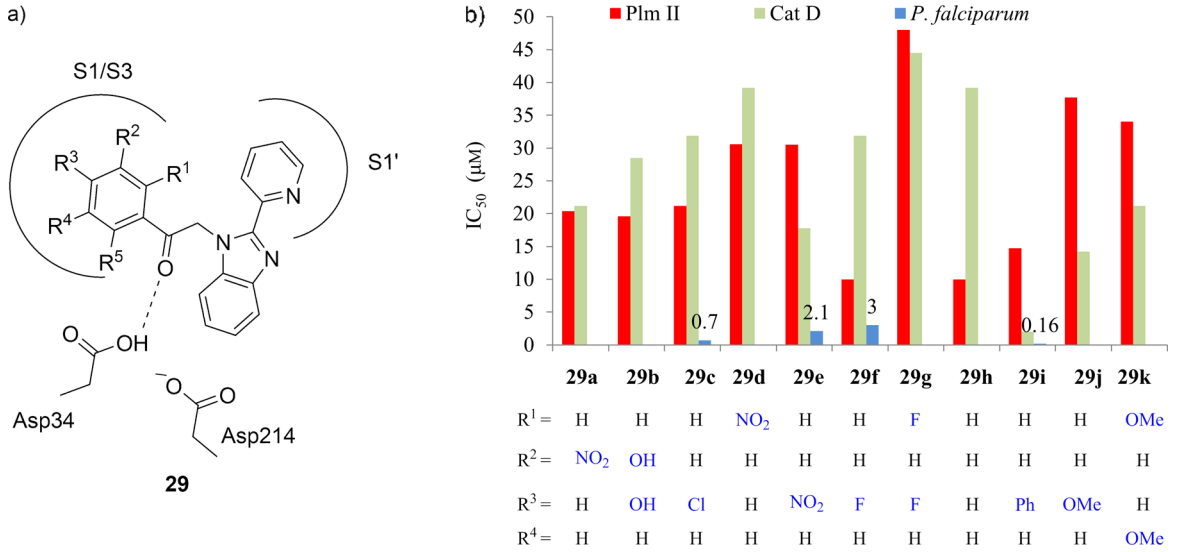

Figure 13. Benzimidazole inhibitors reported by Azim et al.: (a) schematic representation of the binding mode of inhibitor **29**; (b) structures and biochemical activities of **29a–k**. The IC_{50} values for *P. falciparum* are displayed in the graph.[64]

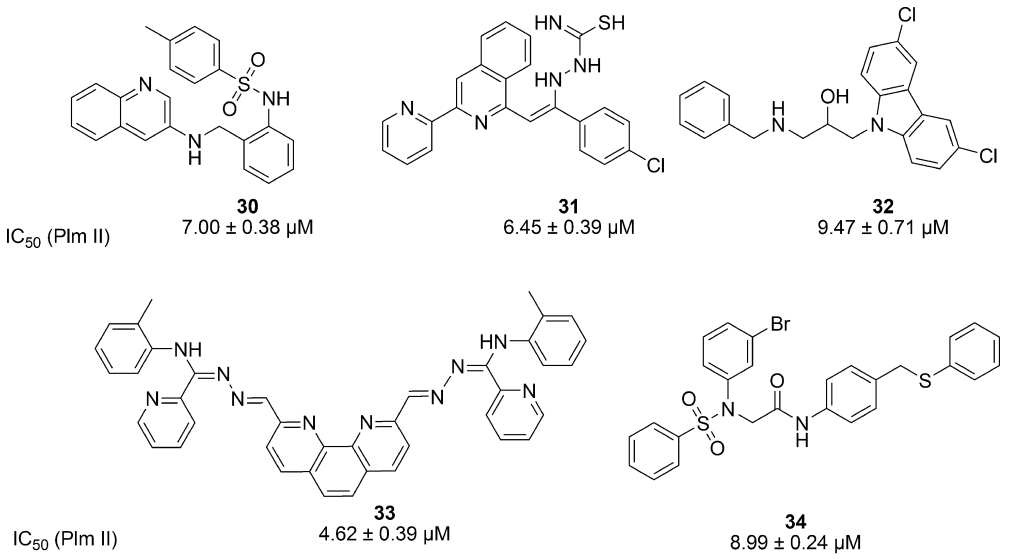

Figure 14. Five new inhibitors reported by Song et al. identified by VS.[65]

and four hydrazide inhibitors (**25–28**, Figure 12c) with micromolar IC_{50} values against Plm II and Cat D.[63] For these small molecules, no specific binding interactions other than those of the scaffold with the catalytic dyad are predicted and it seems probable that they would suffer from selectivity issues. This second series of inhibitors does not constitute an improvement over the previously designed inhibitors (**23a,b**) concerning modeling, selectivity, and activity. To achieve selectivity versus Cat D, the authors suggested varying the heterocyclic substituents for both **23** and **24–28**.

3.4. Benzimidazole Scaffold. In a follow-up study, Azim et al. repeated the same docking procedure of an in-house library, which led to benzimidazole derivatives as potent inhibitors of both Cat D and Plm II.[64] The benzimidazole scaffold contains a pyridine and a benzophenone substituent that are predicted to interact with the S1′ (Tyr192) and S1/S3 (Met15, Ile32, Ser79, and Phe111) pockets, respectively (**29**, Figure 13a). A series of compounds was tested against Plm II and Cat D, showing 2–48 μM activity (Figure 13b). Not many conclusions can be drawn from this series of compounds except that the R^3 substituent seems to affect either Plm II or Plm IV activity. A cell-based assay against *P. falciparum* showed even better activity, with surprisingly low IC_{50} values in the range of 0.16–3 μM (best results were obtained for compounds **29c–i**). Given that these compounds lack selectivity versus Cat D, they cannot be considered promising candidates for the development of novel antimalarials.

3.5. New Inhibitors Identified by VS. In 2013, Song et al. reported a VS of the Specs and Maybridge databases using a crystal structure of Plm II (PDB code 1LEE).[65] Five-hundred compounds were subjected to a visual inspection. Potential inhibitors were selected based on key interactions with the catalytic dyad, flap residues Val78 and Ser79 and with Gly36 and Ser218 (close to the catalytic dyad). 46 (Specs) and 43 (Maybridge) compounds were subjected to biochemical assays. Fifteen compounds suffered from low solubility, but for five compounds (**30–34**) IC_{50} values of <10 μM were obtained (Figure 14). Four different scaffolds were identified with features

DOI: 10.1021/jm5014133
J. Med. Chem. 2015, 58, 5151–5163

similar to those described earlier in this review. Compounds **30** and **34** contain a diamine scaffold with a basic sulfonamide functionality (similar to those described by the group of F. Diederich).[48−50] Compounds **31** and **33** contain hydrazide functionalities (similar to those described by Azim et al.),[61,63] and compound **32** contains an amino alcohol scaffold, which matches the series of inhibitors reported by Friedman and Caflisch.[59]

4. CONCLUSIONS

Much progress has been achieved in SBDD/screening for inhibitors of Plm II. The most important discovery has been the use of flap-pocket substituents to obtain selectivity versus Cat D/E. Especially the group of F. Diederich, who started in 2002 with compounds with low Plm activity ($IC_{50} \geq 4\ \mu M$) and no selectivity versus Cat D/E, has achieved great progress culminating in single-digit nanomolar Plm inhibitors, which are selective versus Cat D/E. The group of Prade has developed the most potent inhibitor, which fulfills the requirements to be an attractive drug candidate (see Introduction): **5** kills the *P. falciparum* parasite (IC_{50} = 45 nM) and is selective versus Cat D and E.

In VS, the issues concerning activity against Plms I−IV and selectivity versus Cat D and E are not always taken into account. For several inhibitors, only IC_{50} values against Plm II are reported (WISDOM project and Song et al.), which is not sufficient. Interesting to note is that although SBDD approaches filling the flap pocket to achieve selective Plm inhibitors, in VS no such approaches have been reported to date. This could explain the difficulty in achieving selectivity versus Cat D/E as experienced by Azim et al. Much insight and information could be gained from VS approaches where flap-pocket substituents are explored. Future VS campaigns may benefit from using models with a focus on crystal structures with the accessible flap pocket to circumvent selectivity issues and to obtain more potent Plm II inhibitors.

Furthermore, it is important to note that excellent activity against Plms in vitro does not ensure success in *P. falciparum* assays. It is thought that this is caused by the fact that several membranes have to be passed before the inhibitor can reach the Plms.[20] On the contrary, some of the less potent Plm inhibitors show high *P. falciparum* activity (Prade and Azim), which could be caused by an unknown mode of action such as inhibition of other *P. falciparum* proteases. However, the unexpected behavior of Plms I−IV inhibitors in *P. falciparum* assays limits the potential of Plm inhibitors as selective, potent drugs and raises questions regarding their mode of action in *P. falciparum*.

In conclusion, SBDD approaches are useful for the development of novel antimalarials agents targeting Plms when taking the following criteria into account: At least three conformationally different crystal structures of Plm II should be used for modeling studies if possible in combination with MD simulations to account for flexibility of the protease.[54] An optimal design should contain a protonated amine functionality ($pK_a > 6$) with aromatic (S1/S3 pocket) or alkyl (flap pocket) substituents for interactions with the lipophilic pockets. Any modeled/screened compound that proves to be potent should be tested against Plms I, II and IV as well as Cat D and E. Selective inhibitors should subsequently be subjected to a *P. falciparum* blood-cell assay. It could also be interesting to focus on differences in inhibition of Plms II and IV in order to determine the similarities and differences of these proteases. Significant differences in activity have been reported in several publications. Following up some of the potent hits discovered by SBVS using SBDD might be an interesting avenue to pursue in the future. A promising approach could be to use scaffolds identified by VS as a starting point for optimization by SBDD taking into account the knowledge available regarding the best substituents.

AUTHOR INFORMATION

Corresponding Author

*Phone: +31 (0)50 363 4275. E-mail: a.k.h.hirsch@rug.nl.

Author Contributions

The manuscript was written through contributions of all authors. All authors have given approval to the final version of the manuscript.

Notes

The authors declare no competing financial interest.

Biographies

Anja P. Huizing studied chemistry at the University of Groningen and obtained her Bachelor's degree in 2012, followed by her Master's degree in 2014. Her Master's research project was supervised by Professor Ben L. Feringa and focused on the synthesis of structurally related amphiphiles using ortho-lithiation strategies and the study of their aggregation with cryo-TEM. She did an internship under the guidance of Professor Philip H. Elsinga, performing research in the field of [^{11}C] and [^{18}F] radiochemistry and PET. In October 2014, she started a Ph.D. under the supervision of Professor Ben L. Feringa and Professor Philip Elsinga on the development and application of bifunctional probes for both MRI and PET.

Milon Mondal obtained his Bachelor of Science in 2008 from the University of Calcutta, Kolkata, India. In 2010, he graduated from the Indian Institute of Technology, Bombay (IIT Bombay), with a Master's degree in Chemistry and pursued his Master's research project under the supervision of Professor M. Ravikanth. Later he joined the group of Professor C. P. Rao at IIT Bombay as a Junior Research Fellow. Since May 2011, he has been working towards his Ph.D. in the Hirsch group on a structure-based design project, in which he combines de novo design with dynamic combinatorial chemistry.

Anna K. H. Hirsch read Natural Sciences with a focus on Chemistry at the University of Cambridge. She spent her third year at the Massachusetts Institute of Technology, doing a research project with Professor Timothy Jamison. She pursued her Master's research project in the group of Professor Steven V. Ley at the University of Cambridge, U.K. She received her Ph.D. from the ETH Zurich in 2008 under the supervision of Professor François Diederich. Subsequently, she joined the group of Professor Jean-Marie Lehn at the Institut de Science et d'Ingénierie Supramoléculaires (ISIS) in Strasbourg, France, as a Postdoctoral Fellow. Since 2010, she has been Assistant Professor at the Stratingh Institute for Chemistry, University of Groningen, The Netherlands. Her work focuses on rational approaches to drug design, exploiting dynamic combinatorial chemistry.

ACKNOWLEDGMENTS

A.K.H.H. received funding from the Ministry of Education, Culture and Science (Gravitation Program 024.001.035).

ABBREVIATIONS USED

Plm, plasmepsin; Cat, cathepsin; SBVS, structure-based virtual screening; SBDD, structure-based drug design; SAR, structure−activity relationship; VS, virtual screening

REFERENCES

(1) WHO. *World Malaria Report*; World Health Organization: Geneva, Switzerland, 2013.

DOI: 10.1021/jm5014133
J. Med. Chem. 2015, 58, 5151−5163

(2) White, N. J. Drug Resistance in Malaria. *Br. Med. Bull.* **1998**, *54*, 703−715.
(3) White, N. J. Review Series Antimalarial Drug Resistance. *J. Clin. Invest.* **2004**, *113*, 1084−1092.
(4) Dondorp, A. M.; Yeung, S.; White, L.; Nguon, C.; Day, N. P. J.; Socheat, D.; von Seidlein, L. Artemisinin Resistance: Current Status and Scenarios for Containment. *Nat. Rev. Microbiol.* **2010**, *8*, 272−280.
(5) Biamonte, M. A.; Wanner, J.; Le Roch, K. G. Recent Advances in Malaria Drug Discovery. *Bioorg. Med. Chem. Lett.* **2013**, *23*, 2829−2843.
(6) Perez, B.; Teixeira, C.; Gomes, J. R. B.; Gomes, P. Development of *Plasmodium falciparum* Protease Inhibitors in the Past Decade (2002−2012). *Curr. Med. Chem.* **2013**, *20*, 3049−3068.
(7) Khan, S. M.; Waters, A. P. Malaria Parasite Transmission Stages: An Update. *Trends Parasitol.* **2004**, *20*, 575−580.
(8) Goldberg, D. E. Hemoglobin Degradation in Plasmodium-Infected Red Blood Cells. *Semin. Cell Biol.* **1994**, *4*, 355−361.
(9) Francis, S. E.; Gulzman, I. Y.; Oksman, A.; Knickerbocker, A.; Mueller, R.; Bryant, M. L.; Sherman, D. R.; Russel, D. G.; Goldberg, D. E. Molecular Characterization and Inhibition of a *Plasmodium falciparum* Aspartic Hemoglobinase. *EMBO J.* **1994**, *13*, 306−317.
(10) Francis, S. E.; Sullivan, D. J., Jr.; Goldberg, D. E. Hemoglobin Metabolism in the Malaria Parasite *Plasmodium falciparum*. *Annu. Rev. Microbiol.* **1997**, *51*, 97−231.
(11) Gluzman, Y.; Francis, S. E.; Oksman, A.; Smith, C. E.; Duffin, K. L.; Goldberg, D. E. Order and Specificity of the *Plasmodium falciparum* Hemoglobin Degradation Pathway. *J. Clin. Invest.* **1994**, *93*, 1602−1608.
(12) Young, J. A.; Winzeler, E. A. Using Expression Information To Discover New Drug and Vaccine Targets in the Malaria Parasite *Plasmodium falciparum*. *Pharmacogenomics* **2005**, *6*, 17−26.
(13) Coombs, G. H.; Goldberg, D. E.; Klemba, M.; Berry, C.; Kay, J.; Mottram, J. C. Aspartic Proteases of *Plasmodium falciparum* and Other Parasitic Protozoa as Drug Targets. *Trends Parasitol.* **2001**, *17*, 532−537.
(14) Coombs, G. H.; Mottram, J. C. Parasite Proteinases and Amino Acid Metabolism: Possibilities for Chemotherapeutic Exploitation. *Parasitology* **1997**, *114* (Suppl.), S61−S80.
(15) Rosenthal, P. J. Proteases of Protozoan Parasites. *Adv. Parasitol.* **1999**, *43*, 105−159.
(16) Banerjee, R.; Liu, J.; Beatty, W.; Pelosof, L.; Klemba, M.; Goldberg, D. E. Four Plasmepsins Are Active in the *Plasmodium falciparum* Food Vacuole, Including a Protease with an Active-Site Histidine. *Proc. Natl. Acad. Sci. U.S.A.* **2002**, *99*, 990−995.
(17) Gulnik, S. V.; Majer, P.; Cachau, E.; Erickson, J. W. Structure and Inhibition of Plasmepsin II, a Hemoglobin-Degrading Enzyme from *Plasmodium falciparum*. *Proc. Natl. Acad. Sci. U.S.A.* **1996**, *93*, 10034−10039.
(18) Dame, J. B.; Yowell, C. A.; Omara−Opeyne, L.; Carlton, J. M.; Cooper, R. A.; Li, T. Plasmepsin IV, the Food Vacuole Aspartic Proteinase Found in all *Plasmodium* Species Infecting Man. *Mol. Biochem. Parasitol.* **2003**, *130*, 1−12.
(19) Silva, A. M.; Lee, A. Y.; Brickson, J. W.; Goldberg, D. E. Structural Analysis of Plasmepsin II: A Comparison with Human Aspartic Proteases. *Adv. Exp. Med. Biol.* **1998**, *436*, 363−373.
(20) Ersmark, K.; Samuelsson, B.; Hallberg, A. Plasmepsins as Potential Targets for New Antimalarial Therapy. *Med. Res. Rev.* **2006**, *26*, 626−666.
(21) Liu, J.; Gluzman, I. Y.; Drew, M. E.; Goldberg, D. E. The Role of *Plasmodium falciparum* Food Plasmepsins. *J. Biol. Chem.* **2005**, *280*, 1432−1437.
(22) Omara-Opeyne, A. L.; Moura, P. A.; Sulsona, C. R.; Bonilla, J. A.; Fujioka, H.; Fiddock, D. A.; Dame, J. B. Genetic Disruption of the *Plasmodium falciparum* Digestive Vacuole Plasmepsins Demonstrates Their Functional Redundancy. *J. Biol. Chem.* **2004**, *279*, 54088−54096.
(23) Liu, J.; Istvan, E. S.; Gluzman, I. Y.; Gross, J.; Goldberg, D. E. *Plasmodium falciparum* Ensures Its Amino Acid Supply with Multiple Acquisition Pathways and Redundant Proteolytic Enzyme Systems. *Proc. Natl. Acad. Sci. U.S.A.* **2006**, *103*, 8840−8845.
(24) Sleebs, B. E.; Lopaticki, S.; Marapana, D. S.; O'Neill, M. T.; Rajasekaran, P.; Gadzik, M.; Gunther, S.; Whitehead, L. W.; Lowes, K. N.; Barford, L.; Hviid, L.; Shaw, P. J.; Hodder, A. N.; Smith, B. J.; Cowman, A. F.; Boddey, J. A. Inhibition of Plasmepsin V Activity Demonstrates Its Essential Role in Protein Export, PfEMP1 Display, and Survival of Malaria Parasites. *PLoS Biol.* **2014**, *12*, e1001897.
(25) Sleebs, B. E.; Gadzik, M.; O'Neill, M. T.; Rajasekaran, P.; Lopaticki, S.; Lackovic, K.; Lowes, K.; Smith, B. J.; Cowman, A. F.; Boddey, J. A. Transition State Mimetics of the *Plasmodium* Export Element Are Potent Inhibitors of Plasmepsin V from *P-falciparum* and *P-Vivax*. *J. Med. Chem.* **2014**, *57*, 7644−7662.
(26) Davies, D. R. The Structure and Functions of the Aspartic Proteinases. *Annu. Rev. Biophys. Chem.* **1990**, *19*, 189−215.
(27) Xie, D.; Gulnik, S.; Collins, L.; Gustchina, E.; Suvorov, L.; Erickson, J. W. Dissection of the pH Dependence of Inhibitor Binding Energetics for an Aspartic Protease: Direct Measurement of the Protonation States of the Catalytic Aspartic Acid Residues. *Biochemistry* **1997**, *36*, 16166−16172.
(28) Friedman, R.; Caflisch, A. The Protonation State of the Catalytic Aspartates in Plasmepsin II. *FEBS Lett.* **2007**, *581*, 4120−4124.
(29) Fairlie, D. P.; Tyndall, J. D. A.; Reid, R. C.; Wong, A. K.; Abbenante, G.; Scanlon, M. J.; March, D. R.; Bergman, D. A.; Chai, C. L. L.; Burkett, B. A. Conformational Selection of Inhibitors and Substrates by Proteolytic Enzymes: Implications for Drug Design and Polypeptide Processing. *J. Med. Chem.* **2000**, *43*, 1271−1281.
(30) Schechter, I.; Berger, A. On the Size of the Active Site in Proteases. I. Papain. 1967. *Biochem. Biophys. Res. Commun.* **2012**, *425*, 497−502.
(31) Valiente, P. A.; Batista, P. R.; Pupo, A.; Pons, T.; Valencia, A.; Pascutti, P. G. Predicting Functional Residues in *Plasmodium falciparum* Plasmepsins by Combining Sequence and Structural Analysis with Molecular Dynamics Simulations. *Proteins* **2008**, *73*, 440−457.
(32) Brinkworth, R. I.; Prociv, P.; Loukas, A.; Brindley, P. J. Hemoglobin-Degrading, Aspartic Proteases of Blood-Feeding Parasites: Substrate Specificity Revealed by Homology Models. *J. Biol. Chem.* **2001**, *276*, 38844−38851.
(33) Protein Data Bank. www.pdb.org.
(34) Liu, P.; Marzahn, M. R.; Robbins, A. H.; Gultierrez-de-Teran, H.; Rodriguez, D.; McClung, S. H.; Stevens, S. M.; Yowell, C. A.; Dame, J. B.; McKenna, R.; Dunn, B. M. Recombinant Plasmepsin I from the Human Malaria Parasite *Plasmodium falciparum*: Enzymatic Characterization, Active Site Inhibitor Design, and Structural Analysis. *Biochemistry* **2009**, *48*, 4086−4099.
(35) Asojo, O. A.; Afonina, E.; Gulnik, S. V.; Yu, B.; Erickson, J. W.; Randad, R.; Medjahed, D.; Silva, A. M. Structures of Ser205 Mutant Plasmepsin II from *Plasmodium falciparum* at 1.8 Å in Complex with the Inhibitors rs367 and rs370. *Acta Crystallogr., Sect. D* **2002**, *58*, 2001−2008.
(36) Asojo, O. A.; Gulnik, S. V.; Afonina, E.; Yu, B.; Ellman, J. A.; Haque, T. S.; Silva, A. M. Novel Uncomplexed and Complexed Structures of Plasmepsin II, an Aspartic Protease from *Plasmodium falciparum*. *J. Mol. Biol.* **2003**, *327*, 173−181.
(37) Prade, L.; Jones, A. F.; Boss, C.; Richard-Bildstein, S.; Meyer, S.; Binkert, C.; Bur, D. X-ray Structure of Plasmepsin II Complexed with a Potent Achiral Inhibitor. *J. Biol. Chem.* **2005**, *280*, 23837−23843.
(38) Boss, C.; Corminboeuf, O.; Grisostomi, C.; Meyer, S.; Jones, A. F.; Prade, L.; Binkert, C.; Fischli, W.; Weller, T.; Bur, D. Achiral, Cheap, and Potent Inhibitors of Plasmepsins I, II, and IV. *ChemMedChem* **2006**, *1*, 1341−1345.
(39) Mehlin, C. Structure-Based Drug Discovery for *Plasmodium falciparum*. *Comb. Chem. High Throughput Screening* **2005**, *8*, 5−14.
(40) Boss, C.; Corminboeuf, O.; Grisostomi, C.; Weller, T. Inhibitors of Aspartic Proteases-Potential Antimalarial Agents. *Expert Opin. Ther. Pat.* **2006**, *16*, 295−317.
(41) Meyers, M. J.; Marvin, J.; Goldberg, D. E. Recent Advances in Plasmepsin Medicinal Chemistry and Implications for Future Antimalarial Drug Discovery Efforts. *Curr. Med. Chem.* **2012**, *12*, 445−455.
(42) Salas, P. F.; Herrmann, C.; Orvig, C. Metallomalarials. *Chem. Rev.* **2013**, *113*, 3450−3492.
(43) Bjelic, S.; Nervall, M.; Gutiérrez-de-Terán, H.; Ersmark, K.; Hallberg, A.; Aqvist, J. Computational Inhibitor Design against Malaria Plasmepsins. *Cell. Mol. Life Sci.* **2007**, *64*, 2285−2305.

DOI: 10.1021/jm5014133
J. Med. Chem. 2015, 58, 5151−5163

(44) Carcache, D. A.; Hörtner, S. R.; Bertogg, A.; Binkert, C.; Bur, D.; Märki, H. P.; Dorn, A.; Diederich, F. De Novo Design, Synthesis and in Vitro Evaluation of a New Class of Nonpeptidic Inhibitors of the Malarial Enzyme Plasmepsin II. *ChemBioChem* **2002**, *3*, 1137−1141.
(45) Oefner, C.; Binggeli, a; Breu, V.; Bur, D.; Clozel, J. P.; D'Arcy, a; Dorn, a; Fischli, W.; Grüninger, F.; Güller, R.; Hirth, G.; Märki, H.; Mathews, S.; Müller, M.; Ridley, R. G.; Stadler, H.; Vieira, E.; Wilhelm, M.; Winkler, F.; Wostl, W. Renin Inhibition by Substituted Piperidines: A Novel Paradigm for the Inhibition of Monomeric Aspartic Proteinases? *Chem. Biol.* **1999**, *6*, 127−131.
(46) Carcache, D. A.; Hörtner, S. R.; Seiler, P.; Diederich, F. Development of a New Class of Inhibitors for the Malarial Aspartic Protease Plasmepsin II Based on a Central 7-Azabicyclo[2.2.1]heptane Scaffold. *Helv. Chim. Acta* **2003**, *86*, 2173−2191.
(47) Carache, D. A.; Hörtner, S. R.; Bertogg, A.; Diederich, F. A New Class of Inhibitors for the Malarial Aspartic Protease Plasmepsin II Based on a Central 11-Azatricyclo[6.2.1.$0^{2,7}$]undeca-2,4,6-triene Scaffold. *Helv. Chim. Acta* **2003**, *86*, 2192−2209.
(48) Hof, F.; Schütz, A.; Fäh, C.; Meyer, S.; Bur, D.; Liu, J.; Goldberg, D. E.; Diederich, F. Starving the Malaria Parasite: Inhibitors Active against the Aspartic Proteases Plasmepsins I, II, and IV. *Angew. Chem., Int. Ed.* **2006**, *45*, 2138−2141.
(49) Zürcher, M.; Diederich, F. Structure-Based Drug Design: Exploring the Proper Filling of Apolar Pockets at Enzyme Active Sites. *J. Org. Chem.* **2008**, *73*, 4345−4361.
(50) Zürcher, M.; Hof, F.; Barandun, L.; Schütz, A.; Schweizer, W. B.; Meyer, S.; Bur, D.; Diederich, F. Synthesis of Exo-3-Amino-7-azabicyclo[2.2.1]heptanes as a Class of Malarial Aspartic Protease Inhibitors: Exploration of Two Binding Pockets. *Eur. J. Org. Chem.* **2009**, *2009*, 1707−1719.
(51) Aureggi, V.; Ehmke, V.; Wieland, J.; Schweizer, W. B.; Bernet, B.; Bur, D.; Meyer, S.; Rottmann, M.; Freymond, C.; Brun, R.; Breit, B.; Diederich, F. Potent Inhibitors of Malarial Aspartic Proteases, the Plasmepsins, by Hydroformylation of Substituted 7-Azanorbornenes. *Chem.—Eur. J.* **2013**, *19*, 155−164.
(52) Eder, J.; Hommel, U.; Cumin, F.; Martoglio, B.; Gerhartz, B. Aspartic Proteases in Drug Discovery. *Curr. Pharm. Des.* **2007**, *13*, 271−285.
(53) Fäh, C.; Hardegger, L. A.; Baitsch, L.; Schweizer, W. B.; Meyer, S.; Bur, D.; Diederich, F. New Organofluorine Building Blocks: Inhibitions of the Malarial Aspartic Protease Plasmepsin II and IV by Alicyclic α,α-Difluoroketone Hydrates. *Org. Biomol. Chem.* **2009**, *7*, 3947−3957.
(54) Luksch, T.; Chan, N.-S.; Brass, S.; Sotriffer, C. A.; Klebe, G.; Diederich, W. E. Computer-Aided Design and Synthesis of Nonpeptidic Plasmepsin II and IV Inhibitors. *ChemMedChem* **2008**, *3*, 1323−1336.
(55) Blum, A.; Bottcher, J.; Heine, A.; Klebe, G.; Diederich, W. E. Structure-Guided Design of C(2)-Symmetric HIV-I Protease Inhibitors Based on a Pyrrolidine Scaffold. *J. Med. Chem.* **2008**, *51*, 2078−2087.
(56) Luksch, T.; Blum, A.; Klee, N.; Diederich, W. E.; Sotriffer, C. A.; Klebe, G. Pyrrolidine Derivatives as Plasmepsin Inhibitors: Binding Mode Analysis Assisted by Molecular Dynamics Simulations of a Highly Flexible Protein. *ChemMedChem* **2010**, *5*, 443−454.
(57) Kasam, V.; Zimmermann, M.; Maass, A.; Schwichtenberg, H.; Wolf, A.; Jacq, N.; Breton, V.; Hofmann-Apitius, M. Design of New Plasmepsin Inhibitors: A Virtual High Throughput Screening Approach on the EGEE Grid. *J. Chem. Inf. Model.* **2007**, *47*, 1818−1828.
(58) Degliesposti, G.; Kasam, V.; Da Costa, A.; Kang, H.-K.; Kim, N.; Kim, D.-W.; Breton, V.; Kim, D.; Rastelli, G. Design and Discovery of Plasmepsin II Inhibitors Using an Automated Workflow on Large-Scale Grids. *ChemMedChem* **2009**, *4*, 1164−1173.
(59) Friedman, R.; Caflisch, A. Discovery of Plasmepsin Inhibitors by Fragment-Based Docking and Consensus Scoring. *ChemMedChem* **2009**, *4*, 1317−1326.
(60) Rinehart, J.; Arnold, J.; Canfield, C. J. Evaluation of 2-Phenanthrene Methanols for Antimalarial Activity in Man WR-122,455 and WR-171,669. *Am. J. Trop. Med. Hyg.* **1976**, *25*, 769−774.
(61) Azim, M. K.; Ahmed, W.; Khan, I. A.; Rao, N. A.; Khan, K. M. Identification of Acridinyl Hydrazides as Potent Aspartic Protease Inhibitors. *Bioorg. Med. Chem. Lett.* **2008**, *18*, 3011−3015.
(62) Jiang, S.; Prigge, S. T.; Wei, L.; Gao, Y.; Hudson, T. H.; Gerena, L.; Dame, J. B.; Kyle, D. E. New Class of Small Nonpeptidyl Compounds Blocks *Plasmodium falciparum* Development in Vitro by Inhibiting Plasmepsins. *Antimicrob. Agents Chemother.* **2001**, *45*, 2577−2584.
(63) Ahmed, W.; Rani, M.; Khan, I. A.; Iqbal, A.; Khan, K. M.; Haleem, M. A.; Kamran Azim, M. Characterization of Hydrazides and Hydrazine Derivatives as Novel Aspartic Protease Inhibitors. *J. Enzyme Inhib. Med. Chem.* **2010**, *25*, 673−678.
(64) Saify, Z. S.; Azim, M. K.; Ahmad, W.; Nisa, M.; Goldberg, D. E.; Hussain, S. A.; Akhtar, S.; Akram, A.; Arayne, A.; Oksman, A.; Khan, I. A. New Benzimidazole Derivatives as Antiplasmodial Agents and Plasmepsin Inhibitors: Synthesis and Analysis of Structure-Activity Relationships. *Bioorg. Med. Chem. Lett.* **2012**, *22*, 1282−1286.
(65) Song, Y.; Jin, H.; Liu, X.; Zhu, L.; Huang, J.; Li, H. Discovery of Non-Peptide Inhibitors of Plasmepsin II by Structure-Based Virtual Screening. *Bioorg. Med. Chem. Lett.* **2013**, *23*, 2078−2082.

DOI: 10.1021/jm5014133
J. Med. Chem. 2015, 58, 5151−5163